

ASME Journal of Manufacturing Science and Engineering Online journal at:

https://asmedigitalcollection.asme.org/manufacturingscience



Hao-Yu Liao

Environmental Engineering Sciences, University of Florida, Gainesville, FL 32611 e-mail: haoyuliao@ufl.edu

Behzad Esmaeilian

Assistant Professor College of Business and Information Science, Tuskegee University, Tuskegee, AL 36088 e-mail: besmaeilian@tuskegee.edu

Sara Behdad¹

Associate Professor Environmental Engineering Sciences, University of Florida, Gainesville, FL 32611 e-mail: sarabehdad@ufl.edu

Automated Evaluation and Rating of Product Repairability Using Artificial Intelligence-Based Approaches

Despite the importance of product repairability, current methods for assessing and grading repairability are limited, which hampers the efforts of designers, remanufacturers, original equipment manufacturers (OEMs), and repair shops. To improve the efficiency of assessing product repairability, this study introduces two artificial intelligence (AI) based approaches. The first approach is a supervised learning framework that utilizes object detection on product teardown images to measure repairability. Transfer learning is employed with machine learning architectures such as ConvNeXt, GoogLeNet, ResNet50, and VGG16 to evaluate repairability scores. The second approach is an unsupervised learning framework that combines feature extraction and cluster learning to identify product design features and group devices with similar designs. It utilizes an oriented FAST and rotated BRIEF feature extractor (ORB) along with k-means clustering to extract features from teardown images and categorize products with similar designs. To demonstrate the application of these assessment approaches, smartphones are used as a case study. The results highlight the potential of artificial intelligence in developing an automated system for assessing and rating product repairability. [DOI: 10.1115/1.4063561]

Keywords: machine learning, repairability scores, remanufacturing, automated scoring systems, sustainable manufacturing

1 Introduction

Extending the product lifecycle through repair and reuse is regarded as a sustainability cornerstone. This is particularly important for resource-intensive products such as consumer electronics that require a wide range of rare earth elements in their production. As initiatives such as right-to-repair, promotion of last-longing devices, and consumers' expectation of green products take momentum, it becomes essential to equip designers, manufacturers, and consumers with proper tools to evaluate the degree and extent of product repairability.

In addition, enhancing product repair and reuse is essential for addressing the digital divide problem. The digital divide is one of the country's most pressing, deeply rooted, and often neglected problems [1]. It is estimated that 27% of Americans are on the wrong side of the digital divide due to no internet connectivity or limited access to computer devices. In Fall 2020, at the start of the COVID-19 pandemic, when most Americans began working remotely, 5 million students did not have access to electronic devices for completing schoolwork. Enabling the repair industry is a promising approach to addressing the digital inequalities for students and the 45% of senior citizens who do not own a laptop or PC, or anyone who needs an affordable device [2]. Recently,

28 states filed right-to-repair bills and other repair-related initiatives and demanded set minimum design requirements for manufacturers. The purpose is to develop a legal framework that forces manufacturers to give access to repair manuals and make spare parts available or even at the time of purchase provide customers with information about how long the spare parts will be available in the market [3–5].

However, there is a lack of consistent methods to help manufacturers assess and rate the repairability of their products. Repair is a complex multivariable problem influenced by design, workforce, and market factors. Designers do not have the required tools to evaluate the ease of repair by the workforce and the degree of repairability. Designers have started incorporating design-for-X strategies such as design for disassembly and repair into consideration when evaluating design alternatives. Product design affects the difficulty of repair [6] and influences the steps of disassembling [7], and the efficiency of the entire waste management process [8]. Besides designers, repair shops and remanufacturers also require tools to help them sort recoverable devices and deal with a wide range of end-of-use (EoU) products received in their plants. Also, in many cases, original equipment manufacturers (OEMs) do not share the product repair instructions and it is quite challenging for repair shops to handle different brands of products when dealing with different designs. Many factors such as reliability [9], disassembly [10], and even the choice of business models [11] influence repairability.

The proposed project aims to overcome the gaps in the lack of proper assessment techniques and develop an intelligent scoring

¹Corresponding author.

Manuscript received June 30, 2023; final manuscript received September 20, 2023; published online November 1, 2023. Assoc. Editor: Andy Henderson.

framework by offering a unique way of using machine learning and deep learning techniques. The availability of tools to measure the repairability of devices is crucial for promoting sustainable consumption, reducing waste, and empowering consumers. By accurately assessing the repairability of devices, we can encourage manufacturers to design products that are easier to fix, maintain, and upgrade. These tools enable informed decision-making and empower consumers to choose products that can be repaired with less need for frequent replacements. Further, such scoring systems foster a culture of DIY (Do it Yourself) repairs and skill development and help local repair industries contribute to economic growth and job creation.

The remainder of the paper is organized as follows. Section 2 reviews the related literature. Section 3 describes the proposed frameworks and Sec. 4 discusses the results for the case of smartphone repairability. Finally, Sec. 5 concludes the paper.

2 Background

spare parts to the market [18].

2.1 Product Durability, Longevity, and Repairability. Repair is often acknowledged as a strategy for enhancing environmental sustainability [12]. However, besides environmental benefits, repairable devices reduce the after-sales service cost [13] and are considered among marketing and sales strategies [14], where new service-based business models that are based on sharing and peer economy such as renting, sharing, and exchange would be possible [15]. In addition, repairability is important to future devices' reusability [16] and is a strategy to maintain the source of critical materials and rare earth elements and enhance countries' national security [17]. Recently, independent repair businesses and initiatives have been forming worldwide campaigns to urge manufacturers to produce repairable devices, share repair guides, and supply

Scientific research on the economic aspects of repair is very limited—further, the integration of durability concepts into remanufacturing and design literature is insufficient. The shortcomings of sustainability policies adopted by manufacturers are especially acute in the repairability domain [19]. While different design for X concepts ranging from design for disassembly [20], reliability [21], reuse [22], and recycling [23] have been a part of design efforts, the concept of repairability is one important avenue that is frequently overlooked [24].

2.2 Need for a Repairability Rating System. The lack of repair expertise [25], design guidelines [26], unavailability of spare parts [27], and cost of repair [11] are identified as problematic factors in facilitating repairability. As the recent supply chain disruptions hit the production systems around the globe, the fight for repairable devices gained momentum in Europe, where 38 NGOs across Europe launched the "Right to Repair" campaign to promote repairable design by supporting design practices toward ease of disassembly [28]. The repair campaign emphasizes three initiatives, including the establishment of legislation that sets a minimum requirement for design, forcing OEMs to give access to repair manuals and spare parts, and finally introducing a scoring system for product repairability [29]. Recently the European Commission submitted a standardization request to three European Standardization Organizations, including CEN, CENELEC, and ESTI to support the needs of designing durable products [30]. A joint technical committee was established to develop a series of new standards, including EN 45554:2020 "General methods for the assessment of the ability to repair, reuse and upgrade energy-related products" [31].

Prior studies have discussed key factors for evaluating repairability. To name several studies, Sabbaghi et al. evaluated repairability by surveying consumers' experiences on ease of repair [11]. The ease of disassembly, necessary tools, type of fasteners, availability of spare parts, and documentation were discussed as criteria in the French repair index [32,33]. De Fazio et al. created a disassembly

Table 1 The current repairability scoring mechanisms

Type	Methods	References	
Qualitative methods	iFixit score	[36]	
Semi-quantitative methods	AsMeR RSS PRI	[37,38] [37,39] [40–44]	
Quantitative methods	eDiM	[7,10,45,46]	

map and assessed the ease of disassembly by considering factors such as disassembly sequence, type of tools, fastener, and disassembly time to analyze the repairability of vacuum cleaners [10]. Bracquene et al. discussed scores such as Benelux scores and Austrian durability labels for the repairability of energy-related products [34]. Cordella et al. suggested three levels of assessments including qualitative, semi-quantitative, and quantitative for the assessment of reparability and upgradability [35].

Currently, the repairability assessment methods can be categorized into three groups (Table 1): qualitative, semi-quantitative, and quantitative methods.

The repairability score provided by expert opinions such as the iFixit score is an example of a qualitative scoring system [36]. The semi-quantitative methods are built upon elements such as subjective evaluation criteria and parameter weighting. Examples of semi-quantitative methods include the assessment matrix for ease of repair (AsMeR) [37,38], the repair scoring system (RSS) [5,7], and the priority replacement index (PRI) [40–44]. The quantitative methods on the other hand are based on numerical analysis and mathematical metrics [37]. For instance, the ease of disassembly metric (eDiM) [2,13,14] evaluates the difficulty of disassembly through data measurements.

Although previous literature highlights different criteria and the importance of developing repairability assessment tools, the capabilities of artificial intelligence (AI) models to evaluate repairability have not been explored. The existing evaluation models are resource-intensive and require costly practices.

To comprehensively evaluate the degree of device repairability and better understand the performance of a design in addressing the needs of a workforce with varying repair skills, we will develop a decision-making framework for testing, evaluating, and enhancing repairability using product images. Product teardown data can provide important insights that can help designers and the repair workforce better comprehend and capture the evolving nature of product repairability. Yet our knowledge about the degree of product repairability is limited, and the repair and maintenance workforce cannot comprehend the complexity of the repair process without spending a significant amount of time investigating the device. Very little is currently known about how to identify meaningful patterns in device teardown data and identify how repairable a device is by a medium-skilled workforce. Most importantly, designers do not have the required tools to evaluate the ease of repair by the workforce and the degree of repairability.

To address this gap, this study aims to employ the capabilities of AI technology in assessing product repairability scores. Two frameworks including supervised learning and unsupervised learning are developed. In the supervised learning, deep transfer learning models including ConvNeXt, GoogLeNet, ResNet50, and VGG16 have been applied on a teardown dataset from the iFixit website [36] to link product teardown images to the repairability scores provided by experts' opinions. In the second framework, an unsupervised learning approach that combines oriented FAST and rotated BRIEF (ORB) and k-means clustering is used to conduct similarity analysis among products and assess the repairability score of a device based on its similarity to other existing designs.

To the best of our knowledge, this study is the first one to investigate the ability of AI to develop automatic scoring systems to assess repairability and consequently product maintenance. This

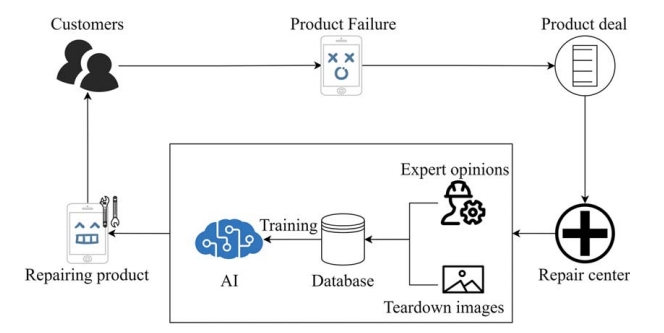


Fig. 1 The Al-driven process to evaluate product repairability

is particularly important for industries such as repair shops and e-waste remanufacturing where refurbishing facilities often receive products with various types, models, and conditions and it is challenging to efficiently separate products based on their future reusability. The proposed AI frameworks trained by experts and teardown images can be employed to evaluate the device condition and finally the decision on whether to repair or not (Fig. 1).

3 The Proposed Repairability Assessment Methods

To investigate the capabilities of AI for repairability assessment, two separate approaches have been investigated. First, a supervised learning framework in which a set of deep learning models are trained by the available repairability scores from repair industry experts. Second, to extend the approach to other designs, an unsupervised learning framework consisting of feature extractor and cluster learning is developed to conduct design similarity analysis.

3.1 The Supervised Learning Framework Based on Object Detection. The proposed automatic repairability system consists of a deep learning model (e.g., ConvNeXt, GoogLeNet, ResNet50, and VGG16) that gets the product teardown image as input and determines the repairability score. The models are trained by labels provided by repair experts. Once the models are trained, they can be used to evaluate the repairability scores for unknown designs. Figure 2 shows an overview of the process.

ConvNeXt, GoogLeNet, ResNet50, and VGG16 are widely recognized deep-learning models renowned for their capabilities in image identification. Among these models, ConvNeXt is a relatively recent addition to the field as it was published in 2022 [47]. ConvNeXt incorporates the design principles of transformers into its architecture to enhance the performance of the classic convolutional neural network [48,49]. Figure 3 depicts the architecture of ConvNeXt, which comprises a ConvNeXt block and a downsample component. Multiple ConvNeXt blocks are stacked within each stage. The final layer is a linear layer that produces the output representing the number of categories.

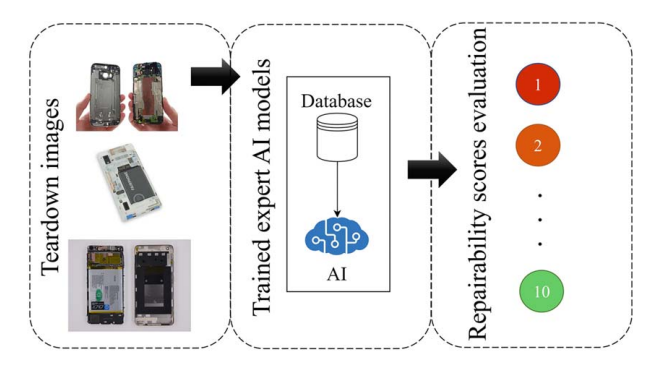


Fig. 2 The supervised learning AI model to evaluate repairability scores from teardown images

GoogLeNet was developed in 2014 [52] and has been trained on over 1 million images from 1000 object types. It has 22 layers including convolution layers, inception layers, max pooling, etc. ResNet50 was developed in 2015 and has 50 layers with 48 convolution layers, 1 max pooling, and 1 average pool layer [53]. Finally, VGG16 was developed in 2014. It has 16 layers and approximately 138 million parameters [54].

In this paper, we have used four well-established pre-trained models (e.g., ConvNeXt, GoogLeNet, ResNet50, and VGG16) using the ImageNet dataset which includes over 1 million labeled images from 1000 classes of objects. Cell phones and mobile phones were among the 1000 classes of objects included in the dataset. Previous studies have already proven the commendable performance of these four models in other applications [47,52–54]. Therefore, we have selected these four models along with the transfer learning to re-train our dataset for the repairability assessment of smartphones.

3.2 The Unsupervised Learning Framework Based on Design Similarity Analysis. This section proposes a framework for identifying and clustering products with similar designs to help repairmen assess the potential repairability of a device based on its similarity to previous designs. Although other economic and market factors such as the availability of spare parts and repair manuals also influence repairability, product design plays a key role in the degree of part accessibility, openability, and disassembly.

The design similarity analysis is conducted solely based on the visual representation of the device in teardown images. We should acknowledge that many criteria such as types of fasteners, types of tools needed, and availability of spare parts are important for repairability [36] which can not necessarily be extracted from product images. Although the similarity analysis does not have detailed information on repairability scores, it still can be a good reference for repairmen to find available repair instructions for newly received products in repair centers.

Figure 4 shows the proposed unsupervised learning framework which consists of an ORB and k-means clustering to analyze design similarity. The ORB extracts features from teardown images and k-means clusters similar designs into the same group.

ORB is more computationally efficient than other extractors such as scale-invariant feature transform and speeded-up robust features [55,56]. ORB uses FAST to find a set of keypoints and applies the Harris corner measure to order the FAST keypoints. Then, the modified version of the descriptor binary robust independent elementary features (BRIEF) is applied to cover FAST keypoints into binary feature vectors that represent the object in the image. The ORB is a data learning model with decent capability in classification problems by finding the keypoint features on images [57].

According to Refs. [56–59], the ORB is built on a descriptor, called the intensity centroid, which measures the corner orientation. The intensity centroid assumes angle intensity is shifted from its center to infer orientation by definition [60]

$$m_{pq} = \sum_{x,y} x^p y^q I(x,y) \tag{1}$$

where m is described as the moments of a patch with sequence p and q, and x, y are the coordinates of pixels in the image. Based on the moments from Eq. (1), the centroid can be obtained as

$$C = \left(\frac{m_{10}}{m_{00}}, \frac{m_{01}}{m_{00}}\right) \tag{2}$$

Then, the angel θ between a vector from the origin to the centroid and x-axis can be expressed as

$$\theta = a \tan 2(m_{01}, m_{10}) \tag{3}$$

where atan2 is the arctangent function with two variables. The x and y are used to measure the moments' region along with the circle area with radius r. The BRIEF descriptor is a set of binary intensity tests

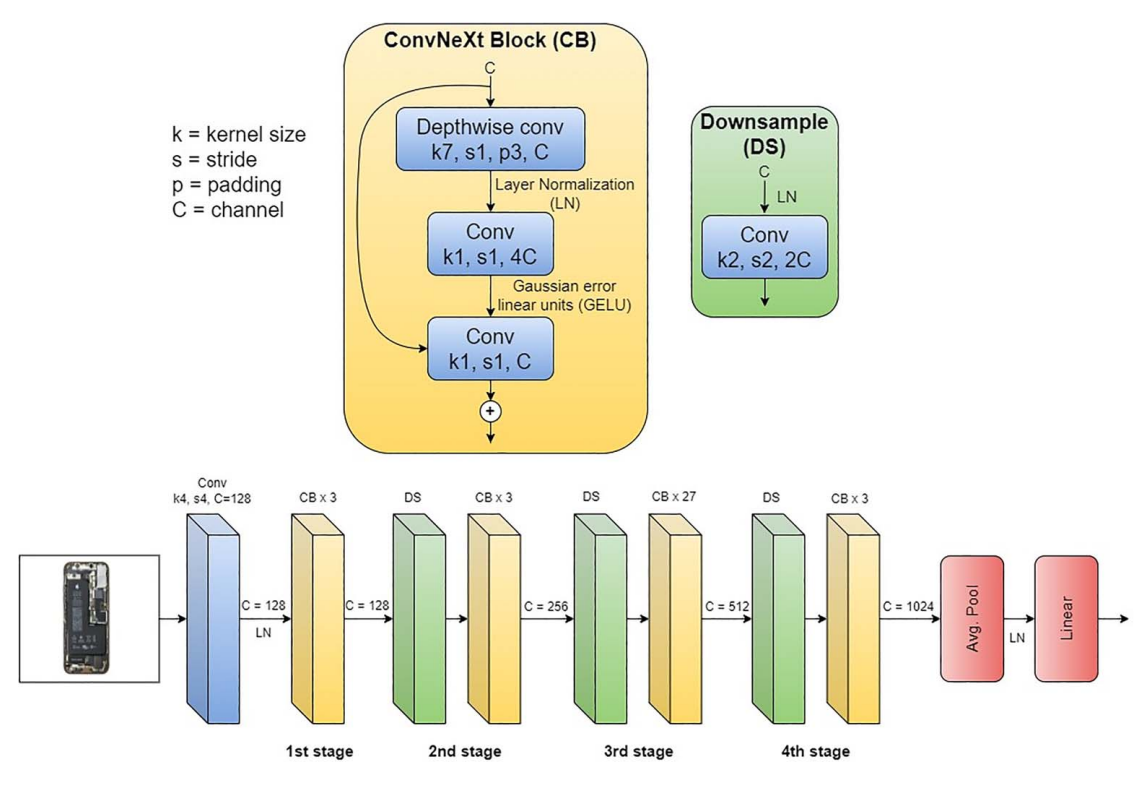


Fig. 3 The ConvNeXt architecture, consists of four stages, each composed of ConvNeXt blocks and a downsample component [50,51]

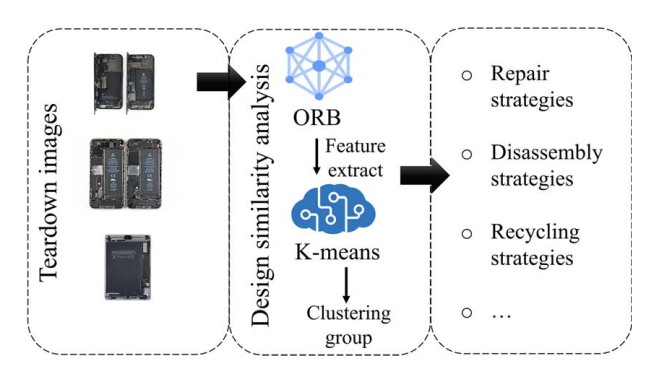


Fig. 4 The proposed framework for design similarity analysis by utilizing teardown images

between an image's pixels [61]. Considering a smoothed patch of image \mathbf{p} , a binary test τ is defined as

$$\tau(\mathbf{p}; x, y) = \begin{cases} 1: \mathbf{p}(x) < \mathbf{p}(y) \\ 0: \mathbf{p}(x) \ge \mathbf{p}(y) \end{cases}$$
(4)

where $\mathbf{p}(x)$ and $\mathbf{p}(y)$ are the intensity of patch \mathbf{p} given points x and y, respectively. The feature is defined to represent the vectors of n binary tests [56]

$$f_n(\mathbf{p}) = \sum_{1 \le i \le n} 2^{i-1} \tau(\mathbf{p}; x_i, y_i)$$
 (5)

where $f_n(p)$ is the descriptor with a vector length of n = 256. Then, the steered BRIEF operator is expressed as

$$g_n(\mathbf{p}, \theta) = f_n(\mathbf{p})|(x_i, y_i) \in S_\theta = R_\theta S$$
 (6)

where S is the feature set of n binary tests at (x_i, y_i) location defined as 2 by n matrix, R_{θ} is the rotation matrix, and S_{θ} is the steered version of S.

K-means is an effective clustering tool still popular [62]. It uses the centroid-based algorithm to find the representative clusters for each group. According to Ref. [63], the objective of k-means clustering is to minimize the following function:

$$J(U) = \sum_{i=1}^{n} \sum_{i=1}^{m} ||x_i - u_i||^2$$
 (7)

where J(U) is the objective function with U as a set of clusters, x_i is the vector sample with n samples, u_j is the jth cluster, and m is the number of clusters. The source codes of this study are available here.²

4 Results and Discussions

In this section, the application of the proposed approaches in the context of smartphones is discussed. Analyses are conducted on two types of images, teardown and X-ray images.

4.1 Repairability Scores of Smartphones

4.1.1 Teardown Images Analysis. To show the application of the proposed supervised learning framework, 945 teardown images of smartphones and their corresponding repairability scores have been collected from the iFixit website. iFixit experts provide a score between 1 and 10 to each device based on criteria such as types of fasteners, necessary tools, modular parts, and the availability of spare parts, to name a few [36]. For instance, a smartphone's repairability score is negatively affected when its outer cover is glued-based and is difficult to open. According to the iFixit scoring rubric, a device gains a high repairability rating when it proves to be easy to disassemble and reassemble, requires minimal costly tools for repair, and facilitates convenient access to critical components [64]. The detailed methodology behind the label generation by experts, the number of experts involved, their

²https://github.com/haoyuliao/AI-Reparability-scores-analysis

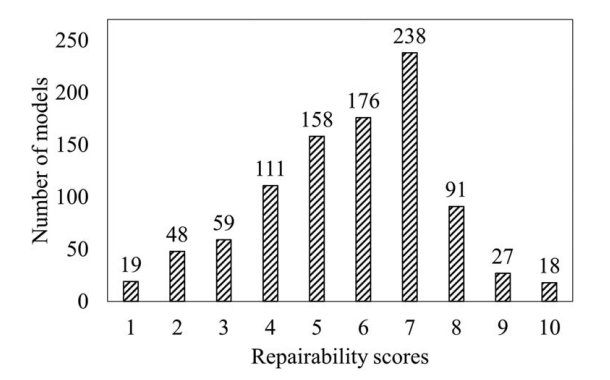


Fig. 5 The distribution of repairability scores of collected images (a total of 945 images)

expertise, and any cross-validation processes remain undisclosed. However, iFixit bases its score assignments on factors such as ease of disassembly, accessibility to components, and the choice of fasteners and joint mechanisms in the design.

The distribution of teardown images and their scores are presented in Fig. 5. 176 and 238 images have repairability scores of 6 and 7, respectively. Only 18 images have a repairability score of 10.

The images are inputs to transfer learning models. In terms of hyperparameters setting, the number of epochs is 100, the batch size is 5, the loss function is cross-entropy, and the decay learning rate is set to 0.1 for every eight epochs with an initial learning rate of 0.001. 80% of teardown images are used for training; 10% for validation; and the remaining 10% for testing. The models' parameters are trained based on training and validation phases, and the testing data as unknown samples are used to further examine the models' performance. In addition, data augmentation is employed during training to further enhance the accuracy.

Besides the 1–10 scale used by iFixit, two more scales are analyzed as listed in Fig. 6. Scale 1 is from 1 to 10 same as iFixit. Scale 2 further combines the 1–10 scores into five classes. Finally, scale 3 combines the scores into three classes: easy repair, medium repair, and hard to repair.

Table 2 shows the score assessment results for the above-mentioned three scales. As expected, the testing accuracy increases as the scale reduces from 10 to 3. Compared to ConvNeXt, GoogLeNet, and VGG16, RestNet50 has higher accuracy on the 3-class scale (88%). Also, as the scales change from 10 to 3 classes, the testing accuracy of ConvNeXt, GoogLeNet, ResNet50, and VGG16 improves from 77% to 82%, from 69% to 87%, from 79% to 88%, and from 70% to 82%, respectively. Although the models are overfitting due to the limited sample size (945), the ResNet50 can still offer 88% accuracy for the 3-class scale in the testing phase.

Figures 7(a)–7(c) show the resulting normalized confusion matrices. As shown, as the scales change from 10 to 3 classes, the accuracy improves. ResNet50 has better accuracy in all scales and offers 88% accuracy in the testing results on the 3-class scale. While ResNet50 has a reasonably good performance, the reason for misclassification is the similarity in teardown images.



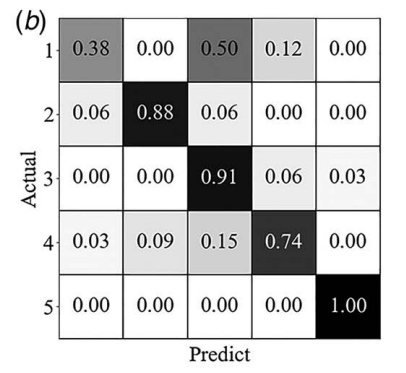
Fig. 6 Three different scales for repairability scores

Table 2 The training, validation, and testing accuracy results of deep learning models on repairability scores

Model	No. of classes	Training accuracy	Validation accuracy	Testing accuracy
ConvNeXt	10	99%	79%	77%
GoogLeNet	10	99%	81%	69%
ResNet50	10	99%	86%	79%
VGG16	10	99%	73%	70%
ConvNeXt	5	99%	78%	77%
GoogLeNet	5	99%	79%	78%
ResNet50	5	97%	77%	80%
VGG16	5	95%	72%	71%
ConvNeXt	3	99%	88%	82%
GoogLeNet	3	99%	88%	87%
ResNet50	3	99%	91%	88%
VGG16	3	98%	83%	82%

(a)	1-	0.33	0.33	0.00	0.00	0.33	0.00	0.00	0.00	0.00	0.00
	2-	0.17	0.33	0.00	0.00	0.17	0.17	0.17	0.00	0.00	0.00
	3-	0.00	0.00	0.86	0.14	0.00	0.00	0.00	0.00	0.00	0.00
	4-	0.00	0.00	0.00	0.83	0.08	0.00	0.00	0.00	0.08	0.00
ual	5-	0.06	0.00	0.00	0.06	0.88	0.00	0.00	0.00	0.00	0.00
Actual	6-	0.00	0.00	0.00	0.00	0.05	0.89	0.00	0.05	0.00	0.00
	7-	0.00	0.04	0.00	0.00	0.00	0.00	0.84	0.08	0.04	0.00
	8-	0.00	0.00	0.10	0.10	0.10	0.00	0.00	0.70	0.00	0.00
	9-	0.00	0.00	0.00	0.00	0.00	0.25	0.00	0.00	0.75	0.00
	10-	0.00	0.00	0.00	0.33	0.00	0.00	0.00	0.00	0.00	0.67

Predict



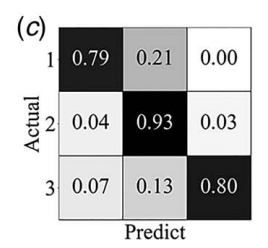


Fig. 7 The normalized confusion matrix for ResNet50 testing results: (a) 79% accuracy for the 10-class scale, (b) 80% accuracy for the 5-class scale, and (c) 88% accuracy for the 3-class scale

(a) ResNet50 evaluating... Actual score: 1 Pred. score: 1

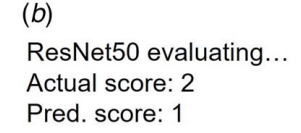






Fig. 8 Repairability scores evaluation by ResNet50 in a 3-class scale in the testing phase for (a) Samsung Galaxy S6 Edge and (b) Samsung Galaxy Note Fan Edition; both are in the same cluster based on similarity assessment

For example, Fig. 8 shows teardowns of the Samsung Galaxy S6 Edge and Samsung Galaxy Note Fan Edition. ResNet50 evaluates the Galaxy S6 Edge score correctly, but the Galaxy Note Fan is miscategorized into Label 1. Comparing the two smartphone models, both have a similar layout such as the position of the camera and

In this study, we applied data augmentation to solve the issues of limited datasets and data imbalance as previous studies highlighted the benefit of data augmentation [65,66].

Despite using data augmentation to mitigate challenges related to limited datasets, the inherent information within the images remains unchanged. As shown in Fig. 5, the majority of the data is concentrated within the range of repairability scores of 4-7. While data augmentation expands the dataset, it does not enhance the original information content. For instance, factors such as the configuration of individual components, the structural attributes of the smartphone, and the dimensions of its constituents remain unchanged, even after applying augmentation techniques such as rotation and horizontal/vertical flips. Consequently, when dealing with a restricted dataset, models are inclined to overfitting, even when we adjust hyperparameters such as learning rate and optimization techniques. Despite the overfitting risk, the models' performance is still reasonable and can achieve up to 88% accuracy on unfamiliar datasets as summarized in Table 2. To address overfitting challenges, future research should focus on the acquisition of additional data.

4.1.2 X-ray Images Analysis. In this study, a total of 66 X-ray images were collected from the iFixit website. These X-ray images provide a comprehensive view of the smartphone's structure without the need for any dismantling. The objective was to assess and compare the model's performance when utilizing X-ray images instead of teardown images.

Figure 9 presents the distribution of repairability scores. Most X-ray images have a repairability score of 6.

When using teardown images as discussed in Sec. 4.1.1, ResNet50 outperforms other models when using the 3-class scale. Therefore, we use the same framework for the X-ray images. The X-ray images are divided into training (80%), validation (10%), and testing (10%). The hyperparameters of ResNet50 are the same as in the previous section. Figure 10 describes the testing results of ResNet50 with an accuracy of 85%.

Figure 11 shows the evaluation results of the testing phase for the teardown image and X-ray image for the Samsung Galaxy Note 20. The utilization of X-ray images provides several advantages compared to teardown images, as it eliminates the need for disassembly actions and offers a clear view of the smartphone's inner structure.

4.1.3 Ablation Study on ResNet50. This section presents an ablation study focusing on ResNet50 for the 3-class scale

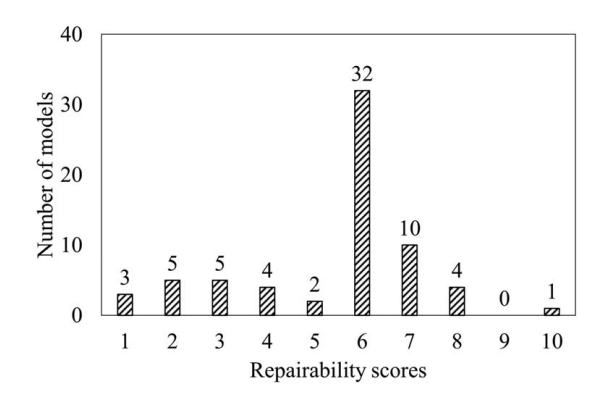


Fig. 9 The distribution of repairability scores of the collected images (a total of 66 images)

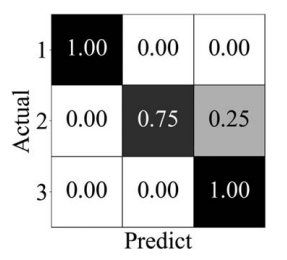


Fig. 10 The normalized confusion matrix of ResNet50 testing results with 85% accuracy for the 3-class scale on X-ray images

(a) (b) ResNet50 evaluating... ResNet50 evaluating... Actual score: 1 Actual score: 1 Pred. score: 1 Pred. score: 1

Fig. 11 Repairability scores evaluation by ResNet50 in a 3-class scale in the testing phase for Samsung Galaxy Note 20: (a) teardown image and (b) X-ray image

prediction, given its performance of achieving a testing accuracy of up to 88%. The purpose of this ablation study is to systematically eliminate specific components of the model and assess their corresponding impacts on overall performance.

ResNet50's architecture consists of four main stages as shown in Fig. 12, where each stage contains convolutional layers [53].

In this study, we explore six modified ResNet50 models, summarized as Ab1-Ab6, which represent the systematic removal of specific stages. These stages are defined as follows: Ab1 (removing the 2nd to 4th stages), Ab2 (removing the 3rd to 4th stages), Ab3 (removing the 1st stage), Ab4 (removing the 2nd stage), Ab5 (removing the 3rd stage), and Ab6 (removing the 4th stage).

Table 3 presents the results of training, validation, and testing accuracy. A decline in accuracy shows the significance of the removed components and their role in the model's overall performance. Particularly, Ab1, Ab2, and Ab6 show lower accuracy, approximately 70%, compared to Ab3-Ab5, which keep an accuracy level of approximately 85%. Among single-stage removal scenarios (Ab3-Ab6), Ab6 shows the lowest accuracy and suggests that the 4th stage holds vital importance in model performance.

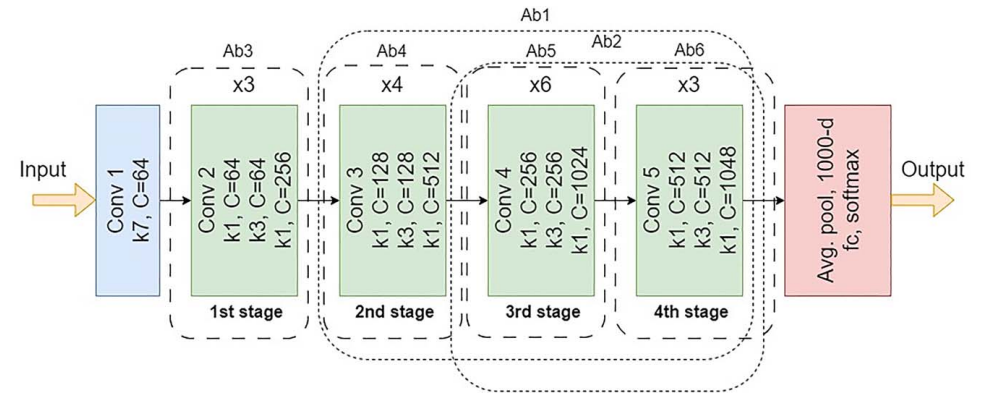


Fig. 12 An overview of the six modified ResNet50 models (Ab1-Ab6: the original ResNet50 architecture shown with a solid line is obtained from Ref. [53]). The dashed line represents the components removed from the original architecture before training.

Table 3 The training, validation, and testing accuracy results of the ablation study on ResNet50 for repairability scores in the 3-class scale

Model	Removal stage	Training accuracy	Validation accuracy	Testing accuracy
Ab1	2nd to 4th	72%	73%	70%
Ab2	3rd to 4th	72%	73%	70%
Ab3	1st	98%	87%	85%
Ab4	2nd	99%	89%	85%
Ab5	3rd	99%	92%	85%
Ab6	4th	72%	73%	70%

Still, the original ResNet50 architecture has the highest testing accuracy of 88% in comparison to Ab1–Ab6. This underlines the non-redundancy of components within ResNet50 and emphasizes the significance of each part. Furthermore, our findings indicate that the 4th stage contributes significantly to model performance which can be investigated further in future studies. One potential future direction is to keep the 4th stage structure and incorporate additional mixed neural network layers to enhance overall accuracy.

4.2 The Similarity of Smartphone Designs. Although supervised learning is capable of properly mapping product images into the repairability score, collecting labeled data, and gathering expert opinions is often very resource-intensive and costly. One solution to address this problem is to identify the similarity of a specific design to existing designs and then infer repairability. To show the feasibility of the proposed approach, 111 teardown images of different brands and models of smartphones have been collected from the iFixit website (Table 4). Each image represents a unique model. Table 4 shows the number of models from each brand with

Table 4 The number of smartphone models from each brand

Brand	Number of models	Brand	Number of models
Samsung	30	Microsoft	1
iPhone	26	Essential	1
Google	8	Meizu	1
Huawei	7	Wiko	1
Motorola	7	Shift	1
Nexus	6	BlackBerry	1
Fairphone	4	Amazon	1
HTĆ	4	Mi	1
LG	3	Nokia	1
Apple	3	Xiaomi	1
OnePlus	3	Total	111

iPhone and Samsung representing the most frequent brands each with 26 and 30 models.

Two teardowns with features such as camera position, component size, and structure are shown in Fig. 8. Each teardown image is resized into 224 by 224 with a grayscale image. Then, ORB retrieves features from each image. The first 250 keypoints are selected from each image. The size of each keypoint is 32 by 1 vector and the size of each input to k-means clustering is 250 by 32. The 250 keypoints of each image are further fed into k-means. Finally, k-means groups images with similar features into the same group.

The best number of clusters is decided by the Dunn index. As shown in Fig. 13, the maximum Dunn index is obtained when the number of clusters equals four.

All 111 images are fed to k-means to identify the best number of clusters by the Dunn index. Table 5 shows the clustering outcomes and the number of models in each cluster. Brands (#12) to (#17) are grouped into Cluster 1. Other brands have appeared in two or more clusters.

Figure 14 illustrates the keypoints of the Huawei Mate 10 Pro, highlighting features such as the camera, microphone, and speaker with a circle. Those keypoints can be further analyzed as shown in Fig. 15 which shows the feature-matching results of devices in the same cluster. Each teardown image retrieved 250 keypoints. The percentage of matching points between the Huawei Mate 10 Pro and LG G6 is 32% (79/250). The more matching keypoints mean a more similar layout in teardown images.

Figure 16 demonstrates the average of matching features of Huawei Mate 10 Pro between other models in different clusters.

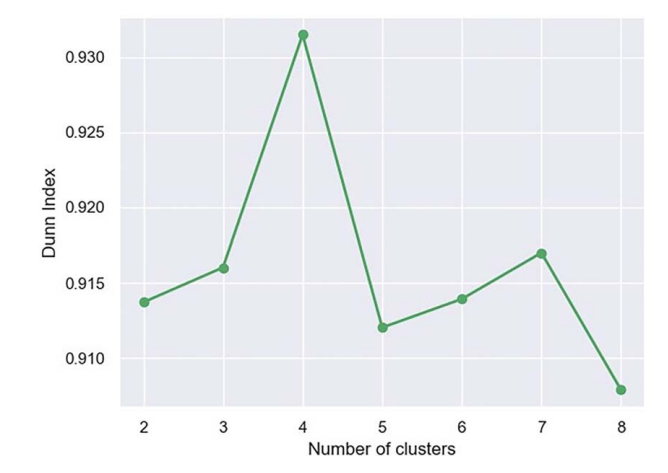


Fig. 13 The Dunn index based on the number of clusters

Table 5 The k-means clustering results

#		Clusters				
	Brand	1	2	3	4	
1	Samsung	13	3	4	10	
2	iPhone	12	8	2	4	
3	Google	4	1	3	0	
4	Huawei	2	4	0	1	
5	Motorola	3	0	1	3	
6	Nexus	1	1	2	2	
7	Fairphone	2	0	1	1	
8	HTĈ	2	0	1	1	
9	LG	1	2	0	0	
10	Apple	1	1	1	0	
11	OnePlus	0	1	1	1	
12	Microsoft	1	0	0	0	
13	Essential	1	0	0	0	
14	Meizu	1	0	0	0	
15	Wiko	1	0	0	0	
16	Shift	1	0	0	0	
17	BlackBerry	1	0	0	0	
18	Amazon	0	1	0	0	
19	Mi	0	0	1	0	
20	Nokia	0	0	1	0	
21	Xiaomi	0	0	0	1	
Total		47	22	18	24	

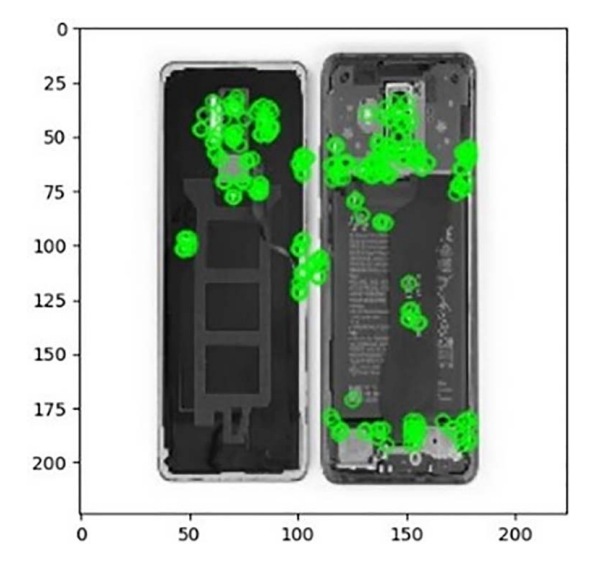


Fig. 14 The results of 250 keypoints from ORB feature extractor on Huawei Mate 10 Pro (with circle)



Fig. 15 The ORB keypoints matching results of Huawei Mate 10 Pro (left) and LG G6 (right) with 79 matching keypoints are in the same cluster

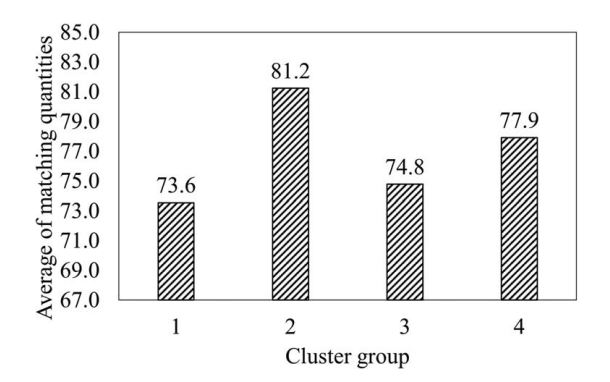


Fig. 16 The average of matching feature quantities between Huawei Mate 10 Pro (belonging to group 2) and all clusters

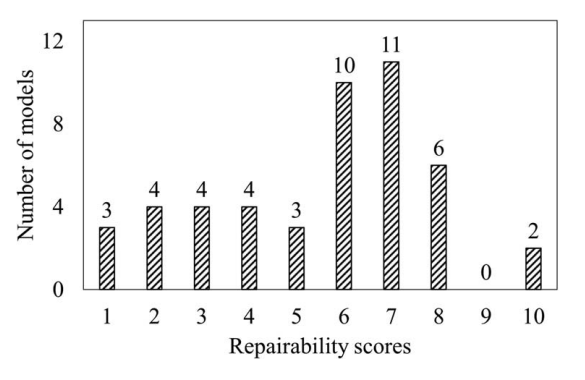


Fig. 17 The distribution of repairability scores of models in cluster 1 (a total of 47 models)

Huawei Mate 10 Pro belongs is assigned to Cluster 2. Note that the highest average matching is 81.2 which is for Cluster 2.

While ORB can find features such as the camera and speaker, it also finds non-meaningful features such as the texts on the battery as shown in Fig. 15. These non-meaningful features, (e.g., the text of the battery), are errors in the k-means. In future research, image segmentation can be applied to first find the specific components such as the camera and speaker, and the non-meaningful segmentation like the text. After filtering, the non-meaningful features using image segmentation, k-means clustering can be used to provide better results.

Figure 17 shows the distribution of repairability scores in Cluster 1. The number of models with a score of 6 and 7 is the most frequent. Despite variation in scores among products within the same cluster, the design similarity analysis highlights promising potential. The results of similarity analysis can help in addressing the lack of repairability information for future designs. It opens up the opportunity for using semi-supervised learning where a limited set of labeled data (e.g., repairability scores from the first section) can be integrated with other unlabeled images from the second section to identify the repairability score of each cluster.

4.3 Implementation of Repairability Analysis in Practice.

To operationalize the proposed frameworks for diverse applications, such as assessing the repairability of automobiles, trucks, and industrial equipment, practical implementation entails several key steps. First, it is necessary to train the models with relevant datasets. The foundation of this process lies in analyzing repairability scores, which are determined based on criteria such as fastener types, required tools, modularity of components, and the availability of spare parts [36]. These repairability scores serve as the ground truth labels during the training of machine learning models. Second, once the repairability scores are carefully defined, an extensive collection of teardown images and sufficient sample size becomes important. The quantity of images becomes a critical factor in effectively associating them with their corresponding repairability scores and using such datasets for training machine learning models. Finally, proper machine learning architecture should be adopted. In this study, we investigated the use of ResNet, VGG, and GoogleNet architectures as the primary models for training the dataset in the smartphone application. However, other capable networks such as Transformers [67], EfficientNet [68], DenseNet [69], Explainable AI [70], and RegNet [71] can be tested for evaluating repairability across various domains.

In terms of computational infrastructure, the models are trained by using a computer desktop with 20 processors (i9-10900 K CPU @ 3.70 GHz), a graphic card (NVIDIA Quadro RTX 4000 GPU), and RAM with 64 GB memory. The parameters of ConvNeXt, GoogLeNet, ResNet50, and VGG16 are 87 M, 5.6 M, 23 M, and 138 M, respectively. The 100 epochs training time of ConvNeXt, GoogLeNet, ResNet50, and VGG16 are 207 min, 31 min, 57 min, and 94 min. Future applications' computational needs may vary based on architectural design, data volume, and specific usage scenarios.

To address data shortage, data augmentation techniques can enhance accuracy by expanding the dataset through methods such as rotation and horizontal/vertical flips. However, it is important to mention that while data augmentation can increase dataset size, obtaining more diverse data remains necessary for improving information diversity.

5 Conclusion

The study investigated two main approaches for assessing product repairability: (1) a deep learning framework that automatically assesses repairability from product teardown images and (2) a design similarity analysis to identify products with similar features and assess repairability based on existing products. The first approach is a supervised learning framework in which four transfer learning models, including ConvNeXt, GoogLeNet, ResNet50, and VGG16, are compared to evaluate the repairability considering three different scales (3, 5, and 10) using teardown images. Besides teardown images, the X-ray images have been applied to demonstrate the proposed framework. The second approach is an unsupervised learning framework that combines ORB feature extractor and k-means clustering to group products with similar designs. The results reveal that ConvNeXt, GoogLe-Net, ResNet50, and VGG16 can have an accuracy of up to 88% for the case of a 3-class scale.

The current study shows several limitations. First, it suffers from data constraints and utilizes only physical images to assess product repairability without considering factors such as product reliability, and electrical and mechanical failures. Future frameworks should incorporate a more extensive scoring system by considering factors beyond just visual inspections. Also, the study relies on teardown and X-ray images, however, product repairability is a complex multidimensional problem. Subsequent research should incorporate various datasets including those that include magnetism and optics features. Moreover, the current dataset is limited and consists of only 111 models from 21 brands. Expanding the dataset to cover a wider collection of brands, product models, and technology types is important for robust findings. In addition, to improve the evaluation accuracy, advanced deep learning models such as transformers and large language models could be employed. These models could consider not only product images but also user queries and feedback to advance the overall assessment.

The study can be extended in several ways. First, the outcomes can be evaluated with expert opinions. Second, the scoring system can be extended to combine the knowledge extracted from object detection with other techniques to tune the repairability scores with other business and sustainability factors. Third, the proposed AI-driven assessment framework can inspire other scores such as disassembly, recyclability, and sustainability in general.

Moreover, the definition of design similarity score can be further extended. Also, the proposed frameworks can be applied to a wide range of product types to identify future research needs.

Acknowledgment

This material is based upon work supported by the National Science Foundation–USA under Grant No. 2026276. Any opinions, findings, conclusions, or recommendations expressed in this material are those of the authors and do not necessarily reflect the views of the National Science Foundation.

Conflict of Interest

There are no conflicts of interest.

Data Availability Statement

The datasets generated and supporting the findings of this article are obtainable from the corresponding author upon reasonable request.

References

- [1] Chakravorti, B., 2021, "How to Close the Digital Divide in the U.S.," Harvard Business Review, https://hbr.org/2021/07how-to-close-the-digital-divide-in-the-
- [2] US PIRG, 2021, "The Costs of the Digital Divide Are Higher Than Ever. Repair Can Help," https://uspirg.org/blogs/blog/usp/costs-digital-di.
- [3] Right to Repair, 2023, 28 States File Right to Repair Legislation and Other Repair Updates.
- [4] US PIRG, 2021, "Half of U.S. States Looking to Give Americans the Right to Repair," https://uspirg.org/blogs/blog/usp/half-us-states-l.
- [5] Gault, M., 2021, "Half the Country Is Now Considering Right to Repair Laws," https://www.vice.com/en/article/z3vavw/half-the-co.
- [6] Bayraktaroglu, S., 2019, Design for Repair as a Strategy to Foster Sustainable User Behavior: A Case of Undergraduate Product Design Studio.
- [7] Vanegas, P., Peeters, J. R., Cattrysse, D., Tecchio, P., Ardente, F., Mathieux, F., Dewulf, W., and Duflou, J. R., 2018, "Ease of Disassembly of Products to Support Circular Economy Strategies," Resour. Conserv. Recycl., 135(June 2017), pp. 323–334.
- [8] van Schaik, A., and Reuter, M. A., 2010, "Dynamic Modelling of E-Waste Recycling System Performance Based on Product Design," Miner. Eng., 23(3), pp. 192–210.
- [9] Cordella, M., Alfieri, F., Clemm, C., and Berwald, A., 2021, "Durability of Smartphones: A Technical Analysis of Reliability and Repairability Aspects," J. Clean. Prod., 286, p. 125388.
- [10] De Fazio, F., Bakker, C., Flipsen, B., and Balkenende, R., 2021, "The Disassembly Map: A New Method to Enhance Design for Product Repairability," J. Clean. Prod., 320, p. 128552.
- [11] Sabbaghi, M., Esmaeilian, B., Cade, W., Wiens, K., and Behdad, S., 2016, "Business Outcomes of Product Repairability: A Survey-Based Study of Consumer Repair Experiences," Resour. Conserv. Recycl., 109, pp. 114–122.
- [12] Wieser, H., and Tröger, N., 2018, "Exploring the Inner Loops of the Circular Economy: Replacement, Repair, and Reuse of Mobile Phones in Austria," J. Clean. Prod., 172, pp. 3042–3055.
- [13] Fang, C.-C., and Hsu, C.-C., 2009, "A Study of Making Optimal Marketing and Warranty Decisions for Repairable Products," 2009 IEEE International Conference on Industrial Engineering and Engineering Management, Hong Kong, China, Dec. 8–11, IEEE, pp. 905–909.
- [14] Gaiardelli, P., Cavalieri, S., and Saccani, N., 2009, "Exploring the Relationship Between After-Sales Service Strategies and Design for X Methodologies," Int. J. Prod. Lifecycle Manag., 3(4), p. 261.
- [15] Preston, F., 2012, Briefing Paper A Global Redesign? Shaping the Circular Economy.
- [16] Cuthbert, R., Giannikas, V., McFarlane, D., and Srinivasan, R., 2016, *Repair Services for Domestic Appliances*, Vol. 640, Springer, Cham, New York, pp. 31–39.
- [17] Peck, D., Kandachar, P., and Tempelman, E., 2015, "Critical Materials From a Product Design Perspective," Mater. Des., 65, pp. 147–159.
- [18] Rosner, D. K., and Ames, M., 2014, "Designing for Repair?" Proceedings of the 17th ACM Conference on Computer Supported Cooperative Work & Social Computing—CSCW '14, New York, NY, Feb. 15–19, pp. 319–331.
- [19] Cairns, C. N., 2005, "E-Waste and the Consumer: Improving Options to Reduce, Reuse and Recycle," Proceedings of the 2005 IEEE International Symposium on Electronics and the Environment, New Orleans, LA, May 16–19, pp. 237–242.
- [20] Harjula, T., Rapoza, B., Knight, W. A., and Boothroyd, G., 1996, "Design for Disassembly and the Environment," CIRP Ann.—Manuf. Technol., 45(1), pp. 109–114.
- [21] Dana, Crowe, 2001, Design for Reliability, CRC Press, Boca Raton, FL.

- [22] Nee, A. Y. C., 2015, Handbook of Manufacturing Engineering and Technology, Springer London, London.
- [23] Gaustad, G., Olivetti, E., and Kirchain, R., 2010, "Design for Recycling," J. Ind. Ecol., 14(2), pp. 286–308.
- [24] Herrmann, J. W., Cooper, J., Gupta, S. K., Hayes, C. C., Ishii, K., Kazmer, D., Sandborn, P. A., and Wood, W. H., 2004, "New Directions in Design for Manufacturing," International Design Engineering Technical Conferences and Computers and Information in Engineering Conference, Salt Lake City, UT, Sept. 28—Oct. 2, pp. 853–861.
- [25] Sabbaghi, M., Cade, W., Behdad, S., and Bisantz, A. M., 2017, "The Current Status of the Consumer Electronics Repair Industry in the US: A Survey-Based Study," Resour. Conserv. Recycl., 116, pp. 137–151.
- Study," Resour. Conserv. Recycl., 116, pp. 137–151.
 [26] Sabbaghi, M., and Behdad, S., 2017, "Optimal Positioning of Product Components to Facilitate Ease-of-Repair," IIE Annual Conference. Proceedings, Institute of Industrial and Systems Engineers (IISE), Pittsburgh, PA, May 20–23, pp. 1000–1005.
- [27] Sabbaghi, M., and Behdad, S., 2018, "Consumer Decisions to Repair Mobile Phones and Manufacturer Pricing Policies: The Concept of Value Leakage," Resour. Conserv. Recycl., 133, pp. 101–111.
- [28] 2020, "Stand up for Your Right to Repair!," https://Repair.Eu/What-We-Want/.
- [29] Bracquene, E., Peeters, J., Duflou, J., and Dewulf, W., 2019, "Developing Repairability Criteria for Energy Related Products: A Case Study for Vacuum Cleaners and Washing Machines," Plate 2019 Conference, Berlin, Germany, Sept. 18–20, pp. 81–85.
- [30] Hughes, R., 2017, "The EU Circular Economy Package-Life Cycle Thinking to Life Cycle Law?," Proc. CIRP, 61, pp. 10-16.
- [31] CENELEC, 2020, "A New Series of European Standards Addresses the Material Efficiency of Energy-Related Products," https://www.cencenelec.eu/, https:// www.cencenelec.eu/news/brief_news/Pages/T.-2020-037.asp.
- [32] Purdy, K., 2021, "Apple Is Using France's New Repairability Scoring—Here's How It Works." iFixit, https://www.ifixit.com/News/49158/france-gave-apple-some-repairability-homework-lets-grade-it.
- [33] Purdy, K., 2021, "Why IFixit's Repair Scores Are Different Than the French Repair Index." iFixit, https://www.ifixit.com/News/49319/why-ifixits-repairscores-are-different-than-the-french-repair-index.
- [34] Bracquene, E., Peeters, J. R., Burez, J., De Schepper, K., Duflou, J. R., and Dewulf, W., 2019, "Repairability Evaluation for Energy Related Products," Proc. CIRP, 80, pp. 536–541.
- [35] Cordella, M., Sanfelix, J., and Alfieri, F., 2018, "Development of an Approach for Assessing the Reparability and Upgradability of Energy-Related Products," Proc. CIRP, 69, pp. 888–892.
- [36] IFixit. "Smartphone Repairability Scores," https://www.ifixit.com/smartphone-repairability.
- [37] Bracquené, E., Peeters, J., Alfieri, F., Sanfélix, J., Duflou, J., Dewulf, W., and Cordella, M., 2021, "Analysis of Evaluation Systems for Product Repairability: A Case Study for Washing Machines," J. Clean. Prod., 281, p. 125122.
- [38] Bracquené, E., Brusselaers, J., Dams, Y., Peeters, J., De Schepper, K., Duflou, J., and Dewulf, W., 2018, "Repairability Criteria for Energy Related Products Study in the BeNeLux Context to Evaluate the Options to Extend the Product Life Time Final Report," Proc. CIRP, 80(June), pp. 536–541.
- [39] Cordella, M., Alfieri, F., and Sanfelix, J., 2019, Analysis and Development of a Scoring System for Repair and Upgrade of Products, Publications Office of the European Union, Luxembourg.
- [40] Mummolo, G., Bari, P., Menolascina, F., Elettrotecnica, I., Orabona, V., Salento, U., Siena, G. P., Ospedale, I., and Sollievo, C., 2007, "A Fuzzy Approach for Medical Equipment Replacement Planning," Proceedings of the Third International Conference on Maintenance and Facility Management, Rome, Italy, Sept. 27–28, pp. 229–235.
- [41] Basiony, M., 2013, "Computerized Equipment Management System," J. Clin. Eng., 38(4), pp. 178–184.
- [42] Taylor, K., and Jackson, S., 2005, "A Medical Equipment Replacement Score System," J. Clin. Eng., 30(1), pp. 37–41.
- [43] Taghipour, S., Banjevic, D., and Jardine, A. K. S., 2011, "Prioritization of Medical Equipment for Maintenance Decisions," J. Oper. Res. Soc., 62(9), pp. 1666–1687.
- [44] Rajasekaran, D., 2005, "Development of an Automated Medical Equipment Replacement Planning System in Hospitals 3.1.4," Proceedings of the IEEE 31st Annual Northeast Bioengineering Conference, Hoboken, NJ, Apr. 2–3, pp. 52–53.
- [45] Vanegas, P., Peeters, J. R., Cattrysse, D., Duflou, J. R., Tecchio, P., Mathieux, F., and Ardente, F., 2016, "Study for a Method to Assess the Ease of Disassembly of Electrical and Electronic Equipment, Method Development and Application to a Flat Panel Display Case Study."
- [46] Peeters, J. R., Tecchio, P., Ardente, F., Vanegas, P., Coughlan, D., and Duflou, J. R., 2018, EDIM: Further Development of the Method to Assess the Ease of Disassembly and Reassembly of Products—Application to Notebook Computers.
- [47] Liu, Z., Mao, H., Wu, C.-Y., Feichtenhofer, C., Darrell, T., and Xie, S., 2022, "A ConvNet for the 2020s," Proceedings of the IEEE/CVF Conference on Computer Vision and Pattern Recognition, New Orleans, LA, June 18–24, pp. 11976– 11986.

- [48] Liu, Z., Lin, Y., Cao, Y., Hu, H., Wei, Y., Zhang, Z., Lin, S., and Guo, B., 2021, "Swin Transformer: Hierarchical Vision Transformer Using Shifted Windows," Proceedings of the IEEE/CVF International Conference on Computer Vision, Montreal, BC, Canada, Oct. 11–17, pp. 10012–10022.
- [49] Zhang, Y., Guo, W., Wu, C., Li, W., and Tao, R., 2023, "FANet: An Arbitrary Direction Remote Sensing Object Detection Network Based on Feature Fusion and Angle Classification," IEEE Trans. Geosci. Remote Sens., 61, pp. 1–11.
- [50] Chen, S., Ogawa, Y., Zhao, C., and Sekimoto, Y., 2023, "Large-Scale Individual Building Extraction From Open-Source Satellite Imagery Via Super-Resolution-Based Instance Segmentation Approach," ISPRS J. Photogramm. Remote Sens., 195, pp. 129–152.
- [51] Fan, J., Zheng, P., and Lee, C. K. M., 2022, "A Multi-granularity Scene Segmentation Network for Human-Robot Collaboration Environment Perception," 2022 IEEE/RSJ International Conference on Intelligent Robots and Systems (IROS), Kyoto, Japan, Oct. 23–27, IEEE, pp. 2105–2110.
- [52] Szegedy, C., Liu, W., Jia, Y., Sermanet, P., Reed, S., Anguelov, D., Erhan, D., Vanhoucke, V., and Rabinovich, A., 2015, "Going Deeper With Convolutions," Proceedings of the IEEE Conference on Computer Vision and Pattern Recognition, Boston, MA, June 7–12, pp. 1–9.
- [53] He, K., Zhang, X., Ren, S., and Sun, J., 2016, "Deep Residual Learning for Image Recognition," Proceedings of the IEEE Conference on Computer Vision and Pattern Recognition, Las Vegas, NV, June 27–30, pp. 770–778.
- [54] Simonyan, K., and Zisserman, A., 2015, "Very Deep Convolutional Networks for Large-Scale Image Recognition," 3rd International Conference on Learning Representations, San Diego, CA, May 7–9.
- [55] Bansal, M., Kumar, M., and Kumar, M., 2021, "2D Object Recognition: A Comparative Analysis of SIFT, SURF and ORB Feature Descriptors," Multimed. Tools Appl., 80(12), pp. 18839–18857.
- [56] Rublee, E., Rabaud, V., Konolige, K., and Bradski, G., 2011, "ORB: An Efficient Alternative to SIFT or SURF," 2011 International Conference on Computer Vision, Barcelona, Spain, Nov. 6–13, pp. 2564–2571.
- [57] Awaludin, M., and Yasin, V., 2020, "Application of Oriented Fast and Rotated Brief (ORB) and Bruteforce Hamming in Library Opency for Classification of Plants," J. Inf. Syst. Appl. Manag. Account. Res., 4(3), pp. 51–59.
- [58] Al-Tamimi, A.-K., Qasaimeh, A., and Qaddoum, K., 2021, "Offline Signature Recognition System Using Oriented FAST and Rotated BRIEF," Int. J. Electr. Comput. Eng., 11(5), p. 4095.
- [59] Sun, Y., Du, G., Lin, Q., Zhong, L., Zhao, Y., Qiu, J., and Cao, Y., 2022, "Individual Wood Board Tracing Method Using Oriented Fast and Rotated Brief Method in the Wood Traceability System," Wood Sci. Technol., 56(3), pp. 1–22.
- [60] Rosin, P. L., 1999, "Measuring Corner Properties," Comput. Vis. Image Underst., 73(2), pp. 291–307.
- [61] Lowe, D. G., 2004, "Distinctive Image Features from Scale-Invariant Keypoints," Int. J. Comput. Vis., 60(2), pp. 91–110.
- [62] Trivedi, V. K., Shukla, P. K., and Pandey, A., 2022, "Automatic Segmentation of Plant Leaves Disease Using Min-Max Hue Histogram and k-Mean Clustering," <u>Multimed. Tools Appl.</u>, 81(14), pp. 1–28.
- [63] Govender, P., and Sivakumar, V., 2020, "Application of k-Means and Hierarchical Clustering Techniques for Analysis of Air Pollution: A Review (1980–2019)," Atmos. Pollut. Res., 11(1), pp. 40–56.
- [64] IFixit. "Understanding 'Provisional' Repairability Scores," https://www.ifixit. com/Wiki/Provisional_Repairability_Scores.
- [65] Shawon, A., Faruk, M. O., Habib, M. B., and Khan, A. M., 2019, "Silicon Wafer Map Defect Classification Using Deep Convolutional Neural Network With Data Augmentation," 2019 IEEE 5th International Conference on Computer and Communications (ICCC), Chengdu, China, Dec. 6–9, IEEE, pp. 1995–1999.
- [66] Hatamian, F. N., Ravikumar, N., Vesal, S., Kemeth, F. P., Struck, M., and Maier, A., 2020, "The Effect of Data Augmentation on Classification of Atrial Fibrillation in Short Single-Lead ECG Signals Using Deep Neural Networks," ICASSP 2020-2020 IEEE International Conference on Acoustics, Speech and Signal Processing (ICASSP), Barcelona, Spain, May 4–8, IEEE, pp. 1264–1268.
- [67] Vaswani, A., Shazeer, N., Parmar, N., Uszkoreit, J., Jones, L., Gomez, A. N., Kaiser, Ł, and Polosukhin, I., 2017, "Attention Is All You Need," Adv. Neural Inf. Process. Syst., 30, pp. 1–11.
- [68] Tan, M., and Le, Q., 2019, "EfficientNet: Rethinking Model Scaling for Convolutional Neural Networks," International Conference on Machine Learning, Long Beach, CA, June 10–15, pp. 6105–6114.
- [69] Huang, G., Liu, Z., Van Der Maaten, L., and Weinberger, K. Q., 2017, "Densely Connected Convolutional Networks," Proceedings of the IEEE Conference on Computer Vision and Pattern Recognition, Honolulu, HI, July 21–26, pp. 4700–4708.
- [70] Gunning, D., Stefik, M., Choi, J., Miller, T., Stumpf, S., and Yang, G.-Z., 2019, "XAI—Explainable Artificial Intelligence," Sci. Rob., 4(37), p. eaay7120.
- [71] Radosavovic, I., Kosaraju, R. P., Girshick, R., He, K., and Dollár, P., 2020, "Designing Network Design Spaces," Proceedings of the IEEE/CVF Conference on Computer Vision and Pattern Recognition, Seattle, WA, June 13–19, pp. 10428–10436.